NATIONAL BUREAU OF STANDARDS REPORT

9451

On the Correlation of Spectral Irradiances
as Determined through the Use of
Prism and Filter Spectroradiometric Techniques

by

William E. Schneider, Ralph Stair, and John K. Jackson
Metrology Division
National Bureau of Standards
Washington, D.C.

Supported by
NASA
Order R-116

NBS

U. S. DEPARTMENT OF COMMERCE
NATIONAL BUREAU OF STANDARDS

THE NATIONAL BUREAU OF STANDARDS

The National Bureau of Standards is a principal focal point in the Federal Government for assuring maximum application of the physical and engineering sciences to the advancement of technology in industry and commerce. Its responsibilities include development and maintenance of the national standards of measurement, and the provisions of means for making measurements consistent with those standards; determination of physical constants and properties of materials; development of methods for testing materials, mechanisms, and structures, and making such tests as may be necessary, particularly for government agencies; cooperation in the establishment of standard practices for incorporation in codes and specifications; advisory service to government agencies on scientific and technical problems; invention and development of devices to serve special needs of the Government; assistance to industry, business, and consumers in the development and acceptance of commercial standards and simplified trade practice recommendations; administration of programs in cooperation with United States business groups and standards organizations for the development of international standards of practice; and maintenance of a clearinghouse for the collection and dissemination of scientific, technical, and engineering information. The scope of the Bureau's activities is suggested in the following listing of its three Institutes and their organizational units.

Institute for Basic Standards. Applied Mathematics. Electricity. Metrology. Mechanics. Heat. Atomic Physics. Physical Chemistry. Laboratory Astrophysics.* Radiation Physics. Radio Standards Laboratory:* Radio Standards Physics; Radio Standards Engineering. Office of Standard Reference Data.

Institute for Materials Research. Analytical Chemistry. Polymers. Metallurgy. Inorganic Materials. Reactor Radiations. Cryogenics.* Materials Evaluation Laboratory. Office of Standard Reference Materials.

Institute for Applied Technology. Building Research. Information Technology. Performance Test Development. Electronic Instrumentation. Textile and Apparel Technology Center. Technical Analysis. Office of Weights and Measures. Office of Engineering Standards. Office of Invention and Innovation. Office of Technical Resources. Clearinghouse for Federal Scientific and Technical Information.**

---

*Located at Boulder, Colorado, 80301.

**Located at 5285 Port Royal Road, Springfield, Virginia, 22171.

NATIONAL BUREAU OF STANDARDS REPORT

NBS PROJECT		NBS REPORT
2120419	October, 1966	9451

On the Correlation of Spectral Irradiances
as Determined through the Use of
Prism and Filter Spectroradiometric Techniques

By
William E. Schneider, Ralph Stair, and John K. Jackson
National Bureau of Standards
Washington, D. C.

Supported by
NASA
Order R-116

NBS

U. S. DEPARTMENT OF COMMERCE

NATIONAL BUREAU OF STANDARDS

NBS Report No. 9451

On the Correlation of Spectral Irradiances as Determined Through the use of Prism and Filter Spectroradiometric Techniques

by

William E. Schneider, Ralph Stair, and John K. Jackson

I. INTRODUCTION

The methods presently employed at the National Bureau of Standards for measuring the spectral irradiances of various sources over the solar spectrum consist of comparing the spectral irradiance of the source under investigation to that of an NBS standard of spectral irradiance. 1/ Two sets of instrumentation 2/, one based on a conventional monochromator and the other a system employing narrow band-pass interference filters to isolate the radiant energy into discrete wavelengths have been set up and independently used in the determination of the spectral irradiances of a number of sources.

In recent years, considerable interest has developed in the methods and techniques employed in the accurate measurement of the spectral energy distribution of various lamp, or arc sources--in particular, over the solar spectrum. The methods principally employed consist of using either: (1) a standard of spectral irradiance, or of spectral radiance 3/ in conjunction with a conventional monochromator, (2) a standard of spectral irradiance, or of spectral radiance along with a set of narrow band-pass interference filters and photoelectric detectors, or (3) a thermal detector which is calibrated through the use of a standard of total irradiance 4,5,6/, or an absolute radiometer 7/ used in conjunction with a set of medium to wide band-pass filters. It is also possible to determine the spectral radiance of tungsten-filament lamps over a limited spectral range by using the published values for the emissivity of tungsten 8,9/ along with a knowledge of the brightness temperature at a particular wavelength 10/, or over the visible range, to calculate the spectral radiant intensity from a knowledge of the luminous intensity and the color temperature. 11/

Variations in the above methods 12,13/ have been made and information has been obtained on the energy distribution of a number of sources. However, little information is available on the absolute correlation of results obtained through the use of two or more of the above methods.

II. Prism Spectroradiometer (Instrumentation)

As shown in Figure 1, the prime component of the "conventional" spectroradiometer is the quartz double-prism monochromator. The use of the double-prism instrument reduces the scattered flux to a minimum and also offers a relatively high degree of resolution. The monochromator is light in weight and compact enabling it to be mounted on a rotary turntable. Thus, the instrument can be rotated to view first one source and then another, one of which is a standard of spectral irradiance. The use of infrasil quartz prisms allows the instrument to be used over the entire spectral range of interest.

In this instrument a single wavelength drum is geared with linkage controls which rotate the two prisms making possible a slow continuous scan through the spectrum. A 3-speed reversible synchronous motor drive has been constructed and geared to the wavelength drum. During each revolution of the wavelength drum three unevenly spaced contacts built into the mechanical drive produce wavelength index marks on the recorder chart. The wavelength calibration of the instrument is performed through the use of known emission lines of various arc lamps.

Since the detectors used with the setup vary significantly in sensitivity over their receiving surfaces and the transmittance of the monochromator varies over its optical aperture, an integrating sphere is placed at the entrance slit of the instrument in order to make sure that the detector always views the same "source." The sphere which is 3 inches in diameter has a circular entrance port (0.75 inch in diameter) and a rectangular (0.75 in by 0.25 in) exit port. The entrance port is situated far enough off the normal to the exit port that it cannot be seen by the detector.

A number of sphere coatings were examined for relative efficiency with the resultant use of MgO reagent grade powder. [14/] The powder is applied to the inner surface of the sphere by merely pressing the powder on the sphere surface by hand and then smoothing over with a fine camel's hair brush. Although the coating is rather fragile, the MgO powder-coated sphere was found to be a factor of at least 2 greater in efficiency than the other sphere coatings tested over the spectral range of about 2.0μ to 2.5μ and equal to, or greater in efficiency than the other coatings over the remainder of the solar spectrum.

Although the reflectance of the MgO powder is quite high (about 98%)[14/], the actual efficiency of the integrating sphere as used with the setup is quite low. The presence of the sphere at the entrance slit of the monochromator reduces the flux as seen by the detector by a factor of at least 1000. Therefore, the detectors and amplifying system must be very sensitive in order to obtain satisfactory results--especially over the UV range from 250 nm to 300 nm and in the infrared beyond 1.5 microns.

Two detectors are employed to cover the entire spectral range from 0.25 to 2.5 microns. An EMI type 9558 QA photomultiplier mounted in a coolable (193°K) housing is used from 0.25μ to 0.8μ, and a 2-mm by 10-mm PbS cell also cooled to 193°K is used from about 0.65 to 2.5 microns. The cooling of the photomultiplier results in an increase in detectivity of about 2 to 3, whereas the detectivity of the cooled PbS cell is a factor of 50 greater than the room temperature PbS cell previously used. Both of the detector housings are constructed to permit either one to be rigidly mounted at the exit slit of the prism instrument. Both horizontal and vertical slots provided on separate mounting plates enable the detectors to be positioned for greatest sensitivity.

Various amplifying systems were tested not only for optimal signal-to-noise ratios, but also for stability and convenience in actual use. The highest signal-to-noise ratios were obtained by using the lock-in type amplifiers.[15,16] Of those examined, the Brower Laboratory Model 129 lock-in amplifier was found to be superior with respect to stability. In actual use the incident flux is chopped at 33 cps and the output of the amplifier is fed directly to a strip-chart recorder which can be operated at a chart speed of 360 inches/hour. The relatively fast chart speed (360 inches/hour) is especially helpful when reducing data obtained on sources containing a number of emission spectra.

In an attempt to reduce stray radiation effects to a minumum, a cylindrical shield (4 1/2 inches in length and 4 1/2 inches in diameter) with a flat black interior surface is mounted to the integrating sphere directly in front of the entrance aperture. The front end of the shield is removable and, depending on the geometry involved, a diaphragm having the appropriate size opening is used. In all cases, however, care must be taken that the limiting aperture of the system is the entrance port of the integrating sphere.

When the spectral irradiance of the standard lamp is compared with that of the source under investigation, large differences in the majority of cases exist between the irradiances of the two sources. These differences can range up to a few orders of magnitude and usually vary with wavelength. Therefore, either a linearity check of the detection system must be performed, or some means of accurately attenuating the more intense source to a value roughly equivalent to that of the other source must be employed.

In our case, it was found both convenient and accurate to use neutral density screens as a means of either performing a linearity check on the detection system, or as a means of obtaining "equivalent" irradiances. The transmittances of the screens were determined through the use of a set of sector disks calibrated by the Length Measurement Section at NBS--with the screens positioned exactly as used. The screens (3" x 3") are placed directly over the opening of the cylindrical shield by sliding the screens into a set of grooves mounted on the shield's diaphragm.

III. Prism Spectroradiometer Measurements

When measurements with the prism instrument are made, the standard of spectral irradiance is placed at a distance of either 50 or 30 cm from the entrance port of the sphere. In most cases a standard calibrated for irradiance at 30 cm is used in order to obtain higher irradiances which are required in the UV and IR for satisfactory signal-to-noise ratios. The spectrometer, along with its auxiliary components, is then rotated to a pre-set position and the source under investigation is then aligned. Measurements are made on each source (standard and unknown) by continuously scanning over the spectral range of each detector. Usually, at least two sets* of curves are obtained on each source.

It is then possible to plot the irradiance of the unknown source as a function of wavelength by reading the data at as many wavelengths as are needed to give a good representation of the "shape" of the irradiance curve. That is, when determining the spectral irradiance of a "line" source, the irradiance is computed every 2 nm in the ultraviolet where the resolution of the monochromator is relatively good (about 1 - 2 nm), every 4 nm in the visible (resolution about 4 - 6 nm), every 10 nm in the IR out to about 1.5μ where the monochromator's resolution becomes increasingly less (from 10 - 50 nm) and every 20 nm from 1.5μ to 2.5μ. By using the irradiance values at these wavelengths and the actual recorder tracings, the spectral irradiance of the unknown source is determined.

The time required to reduce the data is significantly reduced by tabulating the recorder deflection, amplifier gain setting, and the transmittance for each source directly on Fortran coding forms. A typical computer printout for a particular source (BRF-1) over the UV and visible range is shown in Table I. The defining equation for determining the spectral irradiance E_2 at wavelength λ (nm) is given as:

$$E_2 = \frac{E_1 \, D \, G \, \tau_S}{D_S \, G_S \, \tau} \qquad (1)$$

where E_1 = Spectral irradiance of standard, QM-173, (μW cm^{-2} nm^{-1})

D = Recorder deflection for BRF-1

G = Amplifier setting for BRF-1

τ = Transmittance of screen used with BRF-1

D_S = Recorder deflection for QM-173

G_S = Amplifier setting for QM-173

τ_S = Transmittance of screen used with QM-173

The printout is supplemented by a plot of E_2 vs λ as can be seen in Figure 2.

* One set consisting of a complete scan of each source over the entire spectral range 0.25μ - 2.5μ

However, it should be noted that although the resulting curve gives a true representation of the continuum, a true representation of the spectral emission lines is impractical. Since line widths vary considerably, especially when the source is operated at very high pressures, the lines are arbitrarily shown in one of three ways -- namely, as plotted by the particular instrument, as triangles of arbitrary base, or as rectangles of arbitrary base. For most of our work, the first method is used for best representing the data since most of the line sources examined contain spectral lines which are relatively broad or which tend to extend into overlapping bands and also since this method affords greater ease in the reduction of the data.

IV. Photoelectric Filter Spectroradiometer (Instrumentation)

The photoelectric filter spectroradiometer which is shown diagramatically in figure 3 is built around a set of 36 narrow band-pass interference filters which are mounted at 10° intervals on an aluminum disk and which can be rotated by a 36-position T.V. antenna rotor to any one of the 36 positions. A spring and cam arrangement insures that each filter can be positioned directly in front of the detector. A particular filter can be set in position by merely setting a dial to the corresponding filter setting.

Two detectors, an RCA 1P28 photomultiplier and a PbS cell, are mounted on an adjustable table so that by means of an adjustable screw either detector can alternately be brought into proper horizontal position after the dual detector housing is mounted and adjusted for correct vertical positioning.

While it is not absolutely necessary to use an integrating sphere with this instrument, its use is recommended since small errors due to variations in detector surface sensitivity and small errors in determining the true optical distance from the source to detector may occur. A 4" diameter $BaSO_4$ coated integrating sphere having a 3/4" diameter entrance aperture and a 1/2" diameter exit aperture has accordingly been incorporated into the instrument.

In order to eliminate stray radiation, the entire system is enclosed in a light-tight box. Again, to facilitate measurements on the source under investigation and the standard of spectral irradiance, the entire set-up is mounted on an optical bench (lathe bed) and arranged for rapid interchange of position between the two sources.

The electronics employed with the filter set-up along with the read out system, light shield and attenuating screens are identical to those used with the prism spectroradiometer. However, a duplicate chopper is required since the chopper itself is an integral part of both systems.

V. Photoelectric Filter Spectroradiometer (Measurements)

Although the spectral band-passes of the interference filters are relatively narrow as shown in Table 2 for filters representative of various portions of the spectrum, it is necessary to determine the "effective wavelength" for each filter-detector-source combination. From a knowledge of the spectral transmittance of the filter, the relative spectral response of the detector and the relative spectral energy distribution of the source, the effective wavelength λ_{eff} can be calculated through the use of the following equation:

$$\lambda_{eff} = \frac{\int_{\lambda_1}^{\lambda_2} R(\lambda)\ \tau(\lambda)\ E_\lambda\ \lambda\ d\lambda}{\int_{\lambda_1}^{\lambda_2} R(\lambda)\ \tau(\lambda)\ E_\lambda\ d\lambda} \qquad (2)$$

where

λ_{eff} = effective wavelength

$R(\lambda)$ = relative responsivity of detector $(V/(W\ cm^{-2} nm^{-1})$

$\tau(\lambda)$ = spectral transmittance of interference filter

E_λ = relative spectral irradiance of source $(W/cm^2 nm)$

λ = wavelength

The limits of integration λ_1, and λ_2, are taken as the wavelength of 0.1% transmittance.

In most cases the effective wavelength of the standard lamp-filter-detector combination is very nearly equal to that of the unknown source-filter-detector combination throughout the continuum whereas in the vicinity of strong emission lines these differences in λ_{eff} for each source may be significant. However, once the effective wavelength for a particular type of source (filter-detector-source combination) such as a xenon arc lamp has been determined, it is not essential that λ_{eff} be redetermined for other xenon lamps since any differences between the relative energy distribution of the lamps would have to be radical in order to detect any change in λ_{eff}. In tables 3A and 3B are shown the effective wavelengths for a number of filters when used in conjunction with various sources over the photomultiplier spectral range (Table 3A) and when used over the PbS spectral range (Table 3B).

In practice, measurements with the filter spectroradiometer are made with the standard of spectral irradiance at a distance of 50 cm from the entrance port of the sphere. The signal-to-noise ratio when looking at the standard lamp is at least 100 or better at the various wavelengths. The irradiance of the unknown source is compared directly to that of the standard by alternately allowing the filter spectroradiometer to view one source and then the other for each wavelength of interest. The spectral irradiance of the unknown source is given by the following relationship:

$$E'\ (\lambda eff)' = \frac{R_x}{R_{std.}}\ E_{\lambda eff} \qquad (3)$$

where

$E'_{(\lambda eff)'}$ = spectral irradiance at $(\lambda eff)'$ for the unknown source

$E_{\lambda eff}$ = spectral irradiance at λeff for the standard lamp

R_x = detector response for unknown

R_{std} = detector response for standard

The computer printout for a 2500-watt krypton arc when compared to standard QM-173 is shown in Table 4. The parameters E_2, E_1, etc., are identical to those stated in equation 1. However, the irradiance values E_2, should be plotted as a function of the correct effective wavelength, λeff, rather than the nominal wavelength, λ (Column 1, Table 4).

VI. Correlation of Prism Spectroradiometric with Photoelectric Filter Spectroradiometric Results

The spectral irradiances of a number of sources have been measured by using both the prism and filter spectroradiometers and the correlation of the results on a few of the sources measured is shown in Figures 4-10. In all cases, the solid line represents the spectral irradiance as determined through the use of the prism spectroradiometer and the circles are representative of the spectral irradiances as determined with the filter spectroradiometer. The figures are divided into two parts (A and B) with the A section showing the spectral irradiance of the source from 0.25μ to 0.75μ and the B sections from 0.7μ to 2.5μ. Since Figures 4, 5, and 6 are representative of continuous sources, the A sections of these figures have been given two ordinate scales; namely, 0 to 1.8 $\mu W\ cm^{-2}\ nm^{-1}$ from 250 nm to about 340 nm and 0 to 70 $\mu W\ cm^{-2}\ nm^{-1}$ from about 340 nm to 750 nm.

As shown in Figures 4-6, the agreement between the two methods of measurement is very good, the difference being less than 1% in most cases, and the largest difference being about 3%.

When high pressure arc sources are measured, the general agreement of the results between the two methods of measurement is not as good as the agreement for the continuous sources. The results, nevertheless, are encouraging. In Figures 7-10 are shown the spectral irradiances of various high pressure arcs which are representative of the sources commonly used in a number of solar simulators.

In figures 7A and 7B the filter results for the majority of wavelengths on a 2500-watt high pressure xenon arc fall within a couple of percent of the curve derived via the prism instrument. However, there is a 7% discrepancy at 260 nm and a 5% discrepancy at 290 nm. The agreement between the two methods is surprisingly good in the spectral region 0.8μ to 1.5μ where a number of emission bands are present.

In figures 8 to 10 are shown the spectral irradiances of a 2500-watt high pressure HgXe arc and two 2500-watt high pressure krypton arcs. The fact that the correlation of results for the krypton arcs are not as good as the correlation of results for the xenon arc can be attributed primarily to the instability of the krypton arcs.

It should be noted that in the majority of cases in the IR past 1.0 micron, the spectral band-passes of the interference filters are narrower than the band-pass of the monochromator. In the UV and visible, the situation is reversed. This effect is quite noticeable in areas where the filters transmit at wavelengths of strong line emission or if they transmit at wavelengths between two lines that are relatively close to each other. For example, in Figure 8A, the filter set-up gives lower values at the 365 nm, 405 nm and 546 nm emission lines since their resolution is not as good as that of the monochromator. In the IR at 1.1μ, 1.3μ, and 1.5μ (see Figure 8B), the monochromator gives higher values than the filter set-up since these wavelengths are situated between strong emission lines. In the first case, the monochromator values would be more nearly correct, whereas in the second case, the filter values would better represent the actual irradiance of the source.

VII. Concluding Remarks

The close correlation of the spectral irradiances of the sources examined through the use of both the prism spectroradiometer and the photoelectric filter spectroradiometer suggests that repeated spectral energy measurements of solar simulators by using the monochromator method is not always essential. After the spectral irradiance of the solar simulator has been carefully determined by means of the more elaborate prism spectroradiometer, a simple photoelectric filter set-up can be used as the sole instrumentation for periodically checking the irradiance at as many wavelengths as desired.

Efforts are presently being made toward setting up a simple thermoelectric filter spectroradiometer to obtain a third "check" on the photoelectric filter and prism spectroradiometric results. In this case, a "cavity" type [18/] thermopile calibrated in total volts per watt output by means of an N.B.S. tungsten filament lamp standard of total irradiance will be used in conjunction with a set of relatively wide band-pass filters.

References

1/ Ralph Stair, William E. Schneider and John K. Jackson, A New Standard of Spectral Irradiance, Appl. Opt. 2, 1151 (1963).

2/ Ralph Stair, William E. Schneider, William R. Waters, John K. Jackson and Roger E. Brown, Some Developments in Improved Methods For The Measurement of the Spectral Irradiances of Solar Simulators, NASA Report No. CR-201, Washington, D. C. April 1965.

3/ Ralph Stair, Russell G. Johnston and E. W. Halbach, Standard of Spectral Radiance for the Region 0.25 to 2.6 microns, Jr. Res. N.B.S., 64A, 291 (1960).

4/ W.W. Coblentz, Measurements on Standards of Radiation in Absolute Value, Bul, BS 11, 98 (1914) S 227.

5/ W.W. Coblentz and W.B. Emerson, Studies of Instruments for Measuring Radiant Energy in Absolute Value: An Absolute Thermopile, Bul. BS 12, 503 (1916) S 261.

6/ Ralph Stair, William E. Schneider and William B. Fussell, The New Tungsten-Filament Lamp Standards of Total Irradiance, N.B.S. Report No. 9094, April 1966.

7/ Angström, A. K., On Pyrheliometric Measurements, Tellus, 10 No. 3, 342, 1958.

8/ J. C. DeVos, A New Determination of the Emmissivity of Tungsten Ribbon, Physica 20, 690, (1954).

9/ Robert D. Larrabee, Spectral Emissivity of Tungsten, J. Opt. Soc. Am. 49, 619 (1959).

10/ R. Stair and W.O. Smith, A Tungsten-in-Quartz Lamp and Its Applications in Photoelectric Radiometry, J. Research NBS 30, 449 (1943) RP 1543.

11/ Louis E. Barbrow, Memorandum on a Procedure for Obtaining Spectral Radiant Intensity of Tungsten Filament, J. Opt. Soc. Am. 49, 1, 122 (1959).

12/ J.R. Hickey, Correlation of Monochromator and Filter Radiometry Determinations of the Spectral Distribution in Large Solar Simulators, Proceedings IES and ASTM International Symposium on Solar Radiation, Los Angeles, January 1965.

13/ G.C. Goldman, Spectral Measurements by the Filter Method on Lewis' Carbon-Arc Solar Simulators, NASA Lewis Research Center Report, 1964.

14/ David G. Goebel, Patrick B. Caldwell and Harry K. Hammond, III, Use of an Auxiliary Sphere with a Spectroreflectometer to Obtain Absolute Reflectance, J. Opt. Soc. Am. Vol. 56, No. 6, 783 (1966).

15/ Robert D. Moore, Lock-in Amplifiers for Signals Buried in Noise, Electronics 35, No. 23, 40 (June 8, 1962).

16/ R. D. Moore and O. C. Chaykowsky, Modern Signal Processing Technique for Optimal Signal to Noise Ratios, Technical Bulletin 109, Princeton Applied Research Corp., Princeton, N. J., 1963.

17/ John A. Jamieson, Raymond H. McFee, Gilbert N. Plass, Robert H. Grube, Robert G. Richards, Infrared Physics and Engineering, McGraw Hill, 1963.

18/ Ralph Stair and William E. Schneider, Symposium on Thermal Radiation of Solids, San Francisco, California, March 4-6, 1964.

Table 1

BRF-1 VS QM-173
UV AND VIS

LAMBDA	E_1	E.	D	G	T	DS	GS	T_S
250	.05085	.052	6.800	10.000	1.000	6.900	10.000	1.000
260	.08573	.092	18.000	10.000	1.000	19.400	10.000	1.000
270	.15854	.156	49.900	10.000	1.000	49.100	10.000	1.000
280	.23257	.230	54.300	25.000	1.000	53.700	25.000	1.000
290	.38128	.379	66.900	50.000	1.000	66.500	50.000	1.000
300	.55818	.546	77.900	100.000	1.000	76.200	100.000	1.000
310	.76289	.745	72.500	250.000	1.000	70.800	250.000	1.000
320	1.07277	1.040	75.300	500.000	1.000	73.000	500.000	1.000
330	1.46350	1.430	69.900	1000.000	1.000	68.300	1000.000	1.000
340	1.92088	1.900	46.000	2500.000	1.000	45.500	2500.000	1.000
350	2.45017	2.400	29.300	50.000	1.000	28.700	50.000	1.000
360	3.07169	2.980	46.900	50.000	1.000	45.500	50.000	1.000
370	3.86895	3.700	68.700	50.000	1.000	65.700	50.000	1.000
380	4.72979	4.560	97.500	50.000	1.000	47.000	100.000	1.000
390	5.72212	5.480	70.900	100.000	1.000	67.900	100.000	1.000
400	6.72227	6.430	92.000	100.000	1.000	88.000	100.000	1.000
410	7.58305	7.350	42.300	250.000	1.000	41.000	250.000	1.000
420	8.86016	8.580	50.600	250.000	1.000	49.000	250.000	1.000
430	10.24060	9.850	60.300	250.000	1.000	58.000	250.000	1.000
440	11.60346	11.200	71.900	250.000	1.000	69.400	250.000	1.000
450	13.22467	12.700	85.700	250.000	1.000	82.300	250.000	1.000
460	15.19467	14.300	51.800	500.000	1.000	97.500	250.000	1.000
470	16.71261	15.900	61.700	500.000	1.000	58.700	500.000	1.000
480	18.70787	17.600	74.300	500.000	1.000	69.900	500.000	1.000
490	20.49051	19.300	89.500	500.000	1.000	84.300	500.000	1.000
500	22.29167	21.000	53.500	1000.000	1.000	50.400	1000.000	1.000
510	24.15254	22.800	62.500	1000.000	1.000	59.000	1000.000	1.000
520	26.17683	24.700	70.900	1000.000	1.000	66.900	1000.000	1.000
530	28.19022	26.600	78.000	1000.000	1.000	73.600	1000.000	1.000
540	30.11255	28.500	85.900	1000.000	1.000	81.300	1000.000	1.000
550	32.21237	30.400	94.200	1000.000	1.000	88.900	1000.000	1.000
560	34.38797	32.500	40.800	2500.000	1.000	96.400	1000.000	1.000
570	36.87346	34.500	43.500	2500.000	1.000	40.700	2500.000	1.000
580	38.74299	36.400	46.300	2500.000	1.000	43.500	2500.000	1.000
590	41.13704	38.300	49.300	2500.000	1.000	45.900	2500.000	1.000
600	42.98697	40.200	50.900	2500.000	1.000	47.600	2500.000	1.000
610	44.76892	42.100	52.000	2500.000	1.000	48.900	2500.000	1.000
620	46.86179	44.000	52.400	2500.000	1.000	49.200	2500.000	1.000
630	48.69755	45.800	52.100	2500.000	1.000	49.000	2500.000	1.000
640	50.58054	47.500	50.900	2500.000	1.000	47.800	2500.000	1.000
650	52.42670	49.400	48.500	2500.000	1.000	45.700	2500.000	1.000
660	53.49070	51.000	45.100	2500.000	1.000	43.000	2500.000	1.000
670	54.78496	52.800	41.400	2500.000	1.000	39.900	2500.000	1.000
680	55.84696	54.200	37.300	2500.000	1.000	36.200	2500.000	1.000
690	58.17407	55.600	33.900	2500.000	1.000	32.400	2500.000	1.000
700	60.36458	57.000	30.500	2500.000	1.000	28.800	2500.000	1.000
720	62.66638	59.300	24.200	2500.000	1.000	22.900	2500.000	1.000
730	62.95055	60.300	19.000	2500.000	1.000	18.200	2500.000	1.000

Table 2. Filter Band-passes

λ (nm)	Band-pass (nm)
260	20
290	16
360	12
436	5
500	8
600	12
800	19
1000	17
1200	14
1500	14
1800	17
2400	50

Table 3A. Effective Wavelengths of Filters when used with a Photomultiplier and Several Sources

λ_W	λ_{Kr}	λ_{Xe}	λ_{HgXe}
296.6	294.7	294.8	298.2
361.3	361.4	361.4	363.9
391.3	391.0	391.2	390.7
437.0	436.9	437.0	438.1
451.5	451.4	451.5	451.0
550.1	550.2	550.1	549.1
579.0	579.0	579.0	579.2
640.4	640.4	640.3	640.4
680.1	680.0	680.0	680.3

Table 3B. Effective Wavelengths of Filters when used with a PbS Cell and Several Sources

λ_W	λ_{Kr}	λ_{Xe}	λ_{HgXe}
640.8	640.8	640.7	640.8
681.6	681.5	681.4	681.8
699.1	699.1	699.0	699.0
799.6	800.2	800.1	799.7
900.7	900.1	900.6	900.4
1001.6	1001.1	1001.2	1001.8
1193.9	1194.3	1194.0	1194.1
1299.6	1300.0	1299.2	1299.6
1697.8	1698.4	1697.8	1698.9

Table 4

2500-WATT KRYPTON NO. 2 VS QM-173
UV AND VIS AND IR

LAMBDA	E_2	E_1	D	G	T	DS	GS	TS
262	2.41146	.036	90.600	1000.000	.137	9.900	1000.000	1.000
296	2.84778	.172	55.800	2500.000	.137	24.600	2500.000	1.000
300	3.73025	.197	78.000	2500.000	.207	19.900	2500.000	1.000
320	2.91501	.379	72.600	2500.000	.207	45.600	2500.000	1.000
361	5.00701	1.103	63.500	2500.000	.505	27.700	2500.000	1.000
391	5.24825	2.016	98.600	2500.000	.505	75.000	2500.000	1.000
405	5.13411	2.480	57.500	2500.000	.505	55.000	2500.000	1.000
437	7.38426	3.888	75.400	2500.000	.505	39.700	2500.000	.505
451	5.94181	4.651	87.000	2500.000	1.000	68.100	2500.000	1.000
502	5.06144	7.675	88.800	2500.000	1.000	68.000	2500.000	.505
520	5.08960	8.856	68.000	2500.000	.505	48.500	2500.000	.207
546	5.01860	10.690	43.600	2500.000	1.000	46.900	2500.000	.505
550	5.11145	10.960	93.500	2500.000	1.000	41.500	2500.000	.207
579	5.02369	13.030	93.500	1000.000	1.000	50.200	1000.000	.207
599	5.06215	14.440	52.500	1000.000	1.000	31.000	1000.000	.207
6408	5.01963	17.140	68.900	2500.000	1.000	48.700	2500.000	.207
6816	4.33501	19.580	49.200	2500.000	1.000	46.000	2500.000	.207
6991	4.24653	20.450	95.200	1000.000	1.000	94.900	1000.000	.207
641	5.03703	17.140	54.800	100.000	1.000	38.600	100.000	.207
682	4.29350	19.580	62.500	100.000	1.000	59.000	100.000	.207
699	4.18936	20.450	86.100	100.000	1.000	87.000	100.000	.207
800	9.09912	23.510	53.100	500.000	1.000	28.400	500.000	.207
901	7.42837	24.120	91.500	250.000	1.000	61.500	250.000	.207
1001	3.13240	23.510	34.500	250.000	1.000	53.600	250.000	.207
1099	2.71365	22.100	29.600	250.000	1.000	49.900	250.000	.207
1194	3.61514	20.300	81.300	100.000	1.000	94.500	100.000	.207
1300	3.38461	18.220	79.600	100.000	1.000	88.700	100.000	.207
1399	3.08063	16.310	61.500	50.000	1.000	67.400	50.000	.207
1501	1.85036	14.470	50.100	50.000	1.000	81.100	50.000	.207
1598	1.70828	12.740	53.700	50.000	1.000	82.900	50.000	.207
1698	1.82396	11.120	50.000	50.000	1.000	63.100	50.000	.207
1798	1.51374	9.650	41.300	50.000	1.000	54.500	50.000	.207
1900	1.04655	8.350	57.400	50.000	1.000	94.800	50.000	.207
2000	.87873	7.160	45.000	50.000	1.000	75.900	50.000	.207
2100	.79695	6.300	33.000	25.000	1.000	54.000	25.000	.207
2200	.73795	5.580	23.000	100.000	1.000	36.000	100.000	.207
2286	.68214	5.040	20.400	25.000	1.000	31.200	25.000	.207
2394	.69157	4.900	13.500	25.000	1.000	19.800	25.000	.207
2520	.54771	4.030	6.500	25.000	1.000	9.900	25.000	.207

Legends to Illustrations

Figure 1 Optical layout of monochromator and block diagram of prism spectroradiometer.

Figure 2 Computer plot of the spectral irradiance of source BRF-1.

Figure 3 Block diagram of photoelectric filter spectroradiometer.

Figure 4A Spectral irradiance of 1000-watt Quartz Bromine No.1 from 250 nm to 750 nm.

Figure 4B Spectral irradiance of 1000-watt Quartz Bromine No.1 from 0.7μ to 2.5μ.

Figure 5A Spectral irradiance of 1000-watt Frosted Quartz Bromine No.1 from 250 nm to 750 nm.

Figure 5B Spectral irradiance of 1000-watt Frosted Quartz Bromine No.1 from 0.7μ to 2.5μ.

Figure 6A Spectral irradiance of 500-watt Quartz Iodine in aluminum reflector from 250 nm to 750 nm.

Figure 6B Spectral irradiance of 500-watt Quartz Iodine in aluminum reflector from 0.7μ to 2.5μ.

Figure 7A Spectral irradiance of 2500-watt Xenon arc No.1 from 250 nm to 750 nm.

Figure 7B Spectral irradiance of 2500-watt Xenon arc No.1 from 0.7μ to 2.5μ.

Figure 8A Spectral irradiance of 2500-watt HgXe arc No.1 from 250 nm to 750 nm.

Figure 8B Spectral irradiance of 2500-watt HgXe arc No.1 from 0.7μ to 2.5μ.

Figure 9A Spectral irradiance of 2500-watt Krypton arc No.1 from 250 nm to 750 nm.

Figure 9B Spectral irradiance of 2500-watt Krypton arc No.1 from 0.7μ to 2.5μ.

Figure 10A Spectral irradiance of 2500-watt Krypton arc No.2 from 250 nm to 750 nm.

Figure 10B Spectral irradiance of 2500-watt Krypton arc No.2 from 0.7μ to 2.5μ.

Figure 1

PRISM SPECTRORADIOMETER

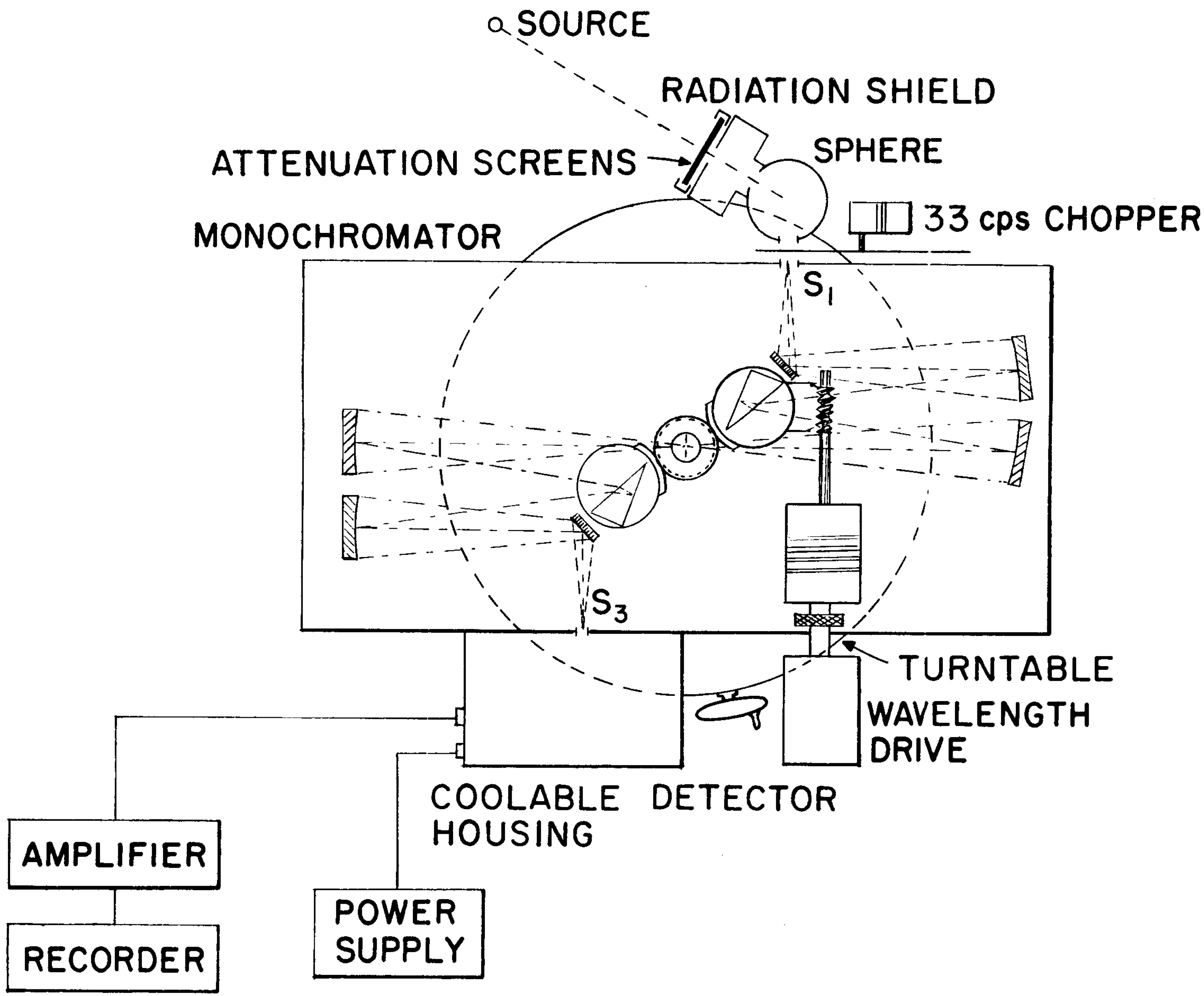

Figure 2

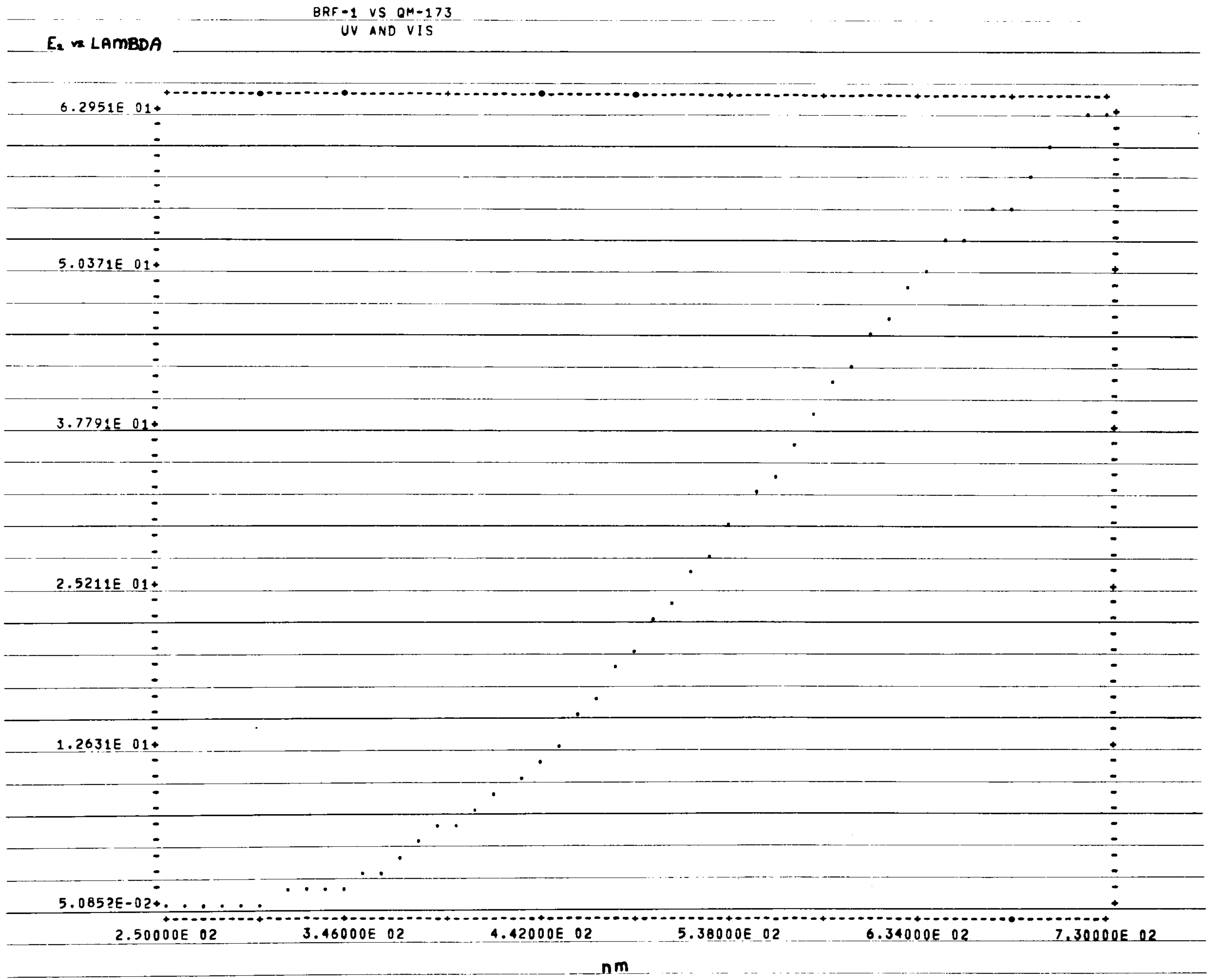

BRF-1 VS QM-173
UV AND VIS
E_2 vs LAMBDA
6.2951E 01
5.0371E 01
3.7791E 01
2.5211E 01
1.2631E 01
5.0852E-02
2.50000E 02
3.46000E 02
4.42000E 02
5.38000E 02
6.34000E 02
7.30000E 02
nm

Figure 3

PHOTOELECTRIC FILTER SPECTRORADIOMETER

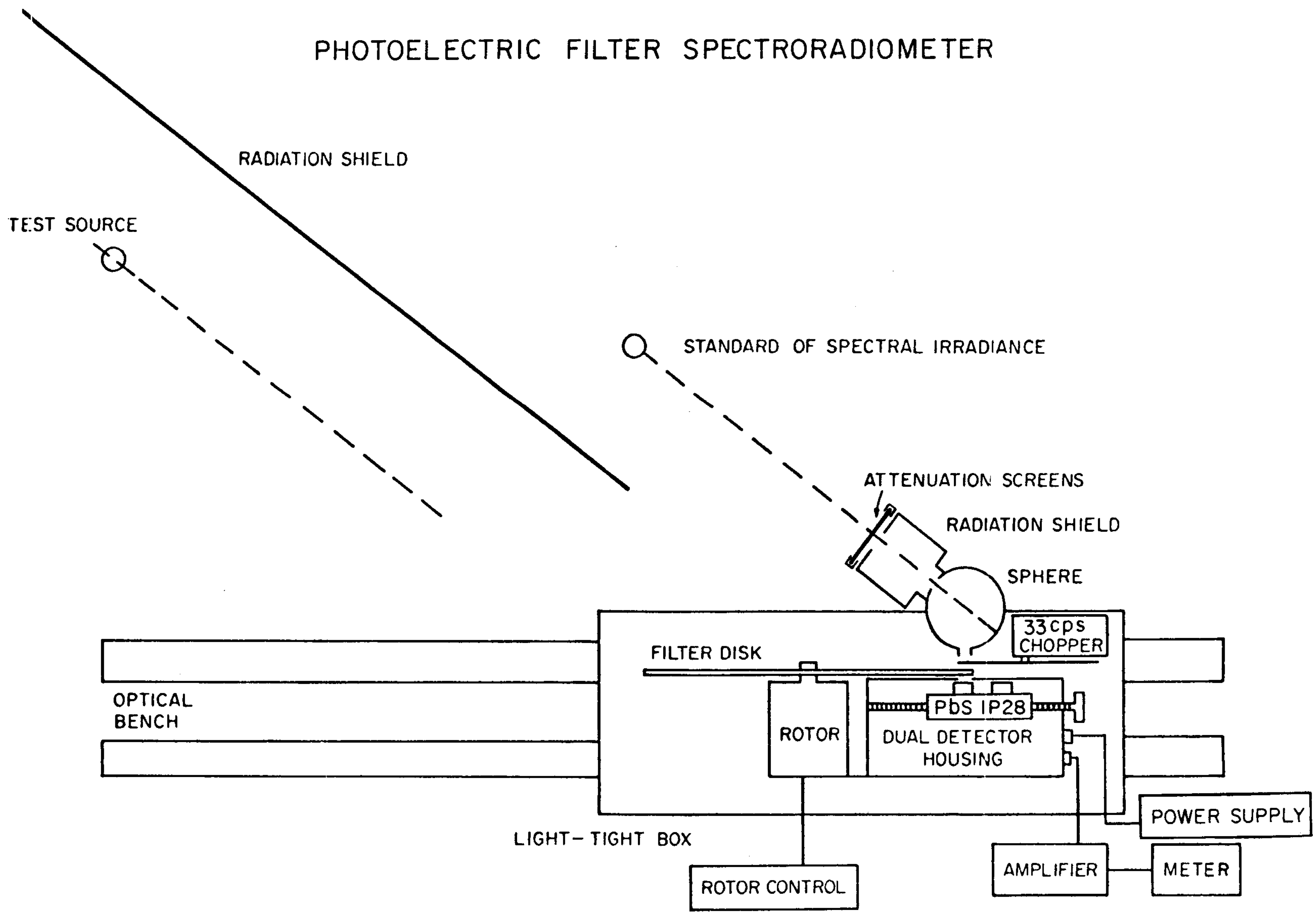

Figure 4A

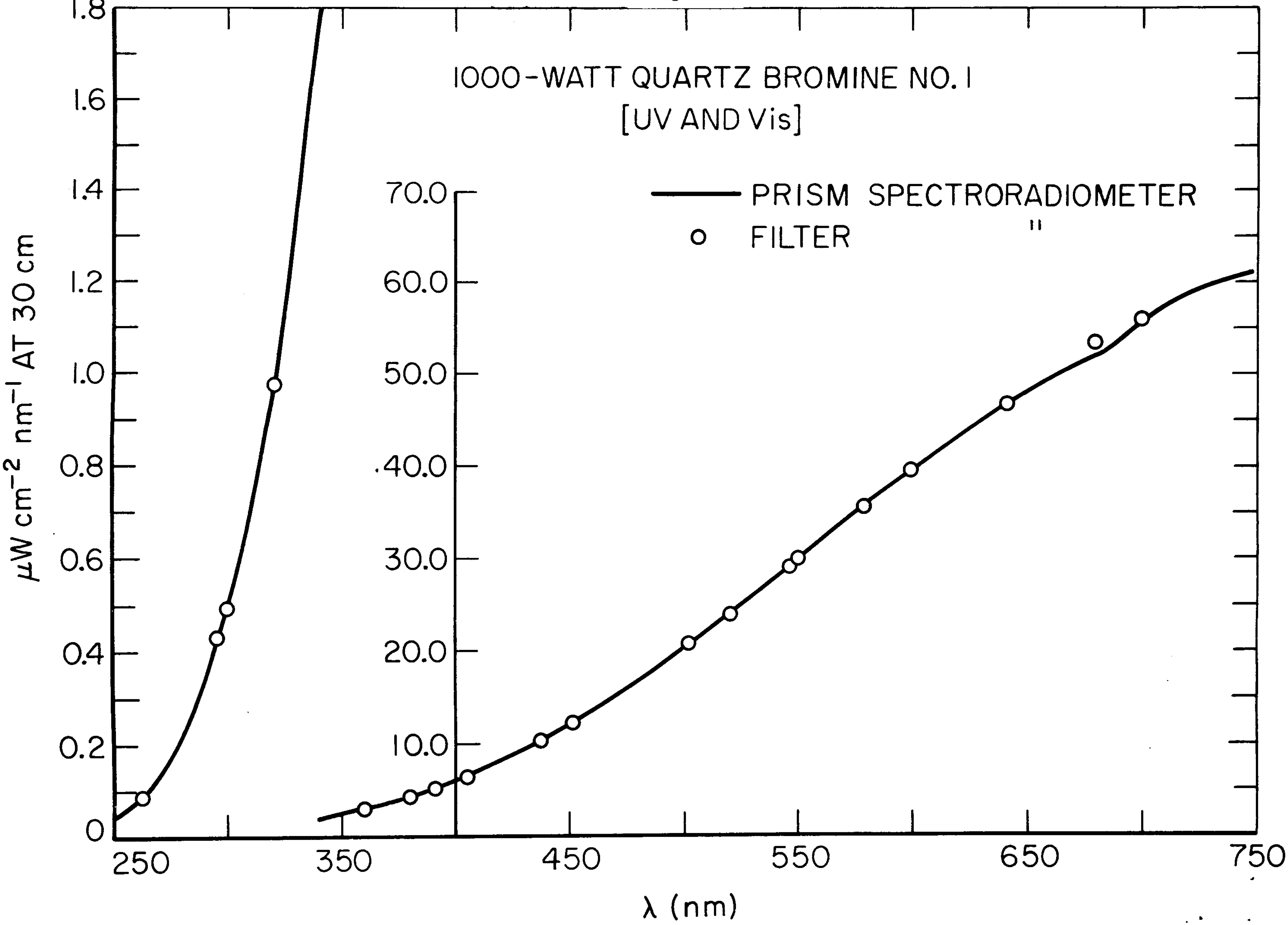
1000-WATT QUARTZ BROMINE NO. 1
[UV AND Vis]
PRISM SPECTRORADIOMETER
FILTER "
μW cm⁻² nm⁻¹ AT 30 cm
λ (nm)
1.8
1.6
1.4
1.2
1.0
0.8
0.6
0.4
0.2
0
70.0
60.0
50.0
40.0
30.0
20.0
10.0
250
350
450
550
650
750

Figure 4B

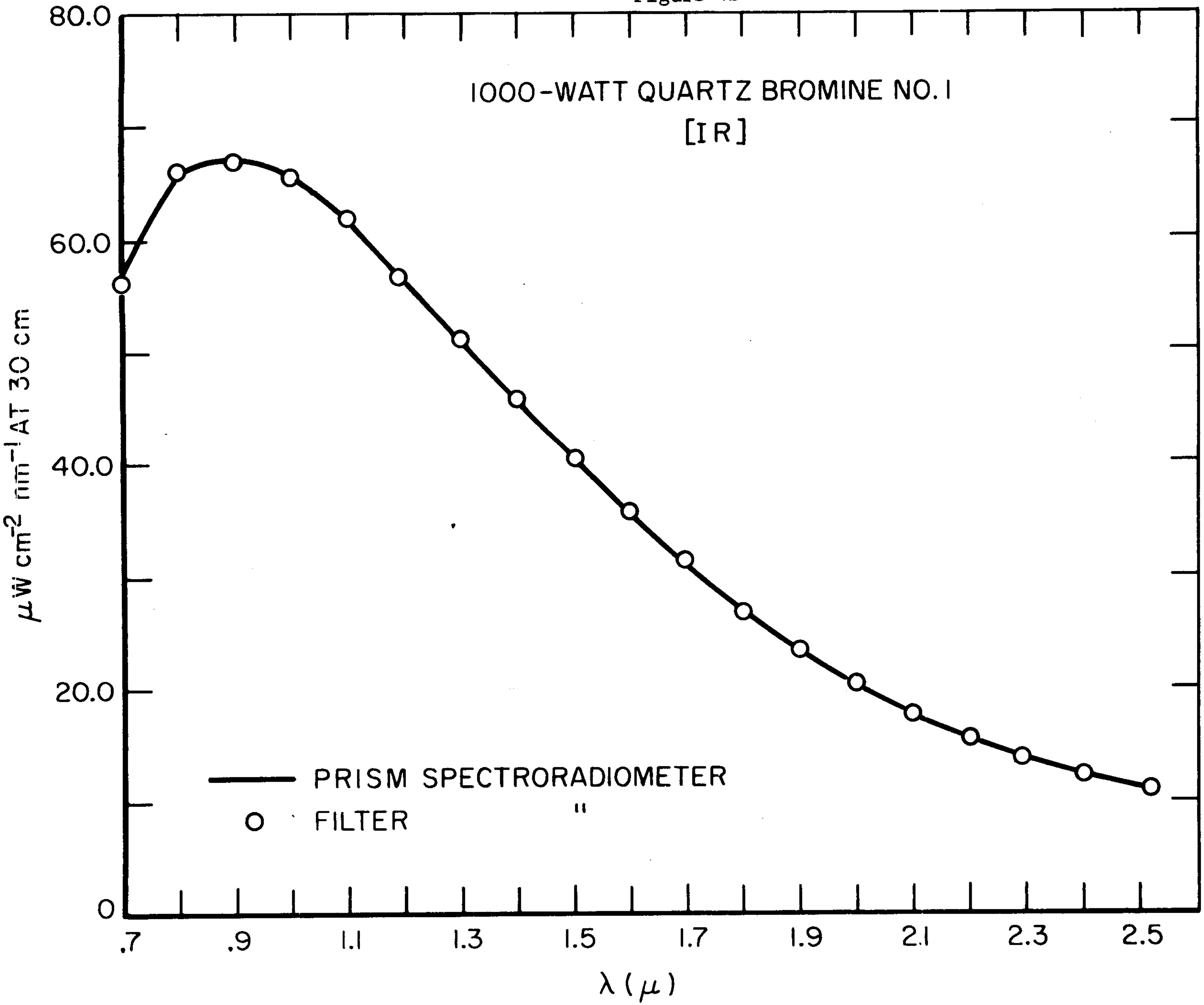
1000-WATT QUARTZ BROMINE NO. 1
[IR]
80.0
60.0
40.0
20.0
0
μW cm⁻² nm⁻¹ AT 30 cm
.7
.9
1.1
1.3
1.5
1.7
1.9
2.1
2.3
2.5
λ (μ)
PRISM SPECTRORADIOMETER
FILTER "

Figure 5A

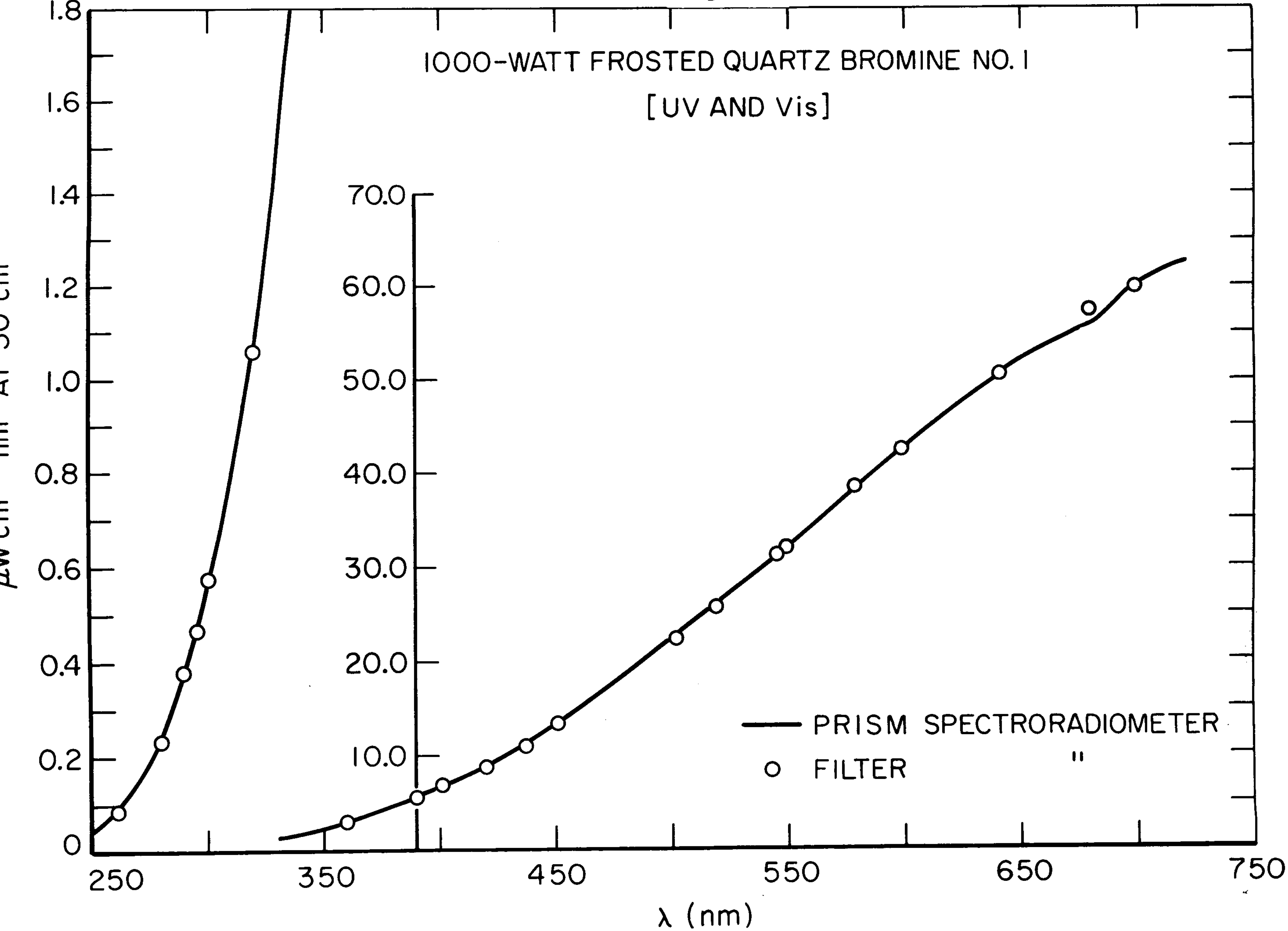
1000-WATT FROSTED QUARTZ BROMINE NO. 1
[UV AND Vis]
PRISM SPECTRORADIOMETER
FILTER "
μW cm⁻² nm⁻¹ AT 30 cm
λ (nm)
1.8
1.6
1.4
1.2
1.0
0.8
0.6
0.4
0.2
0
70.0
60.0
50.0
40.0
30.0
20.0
10.0
250
350
450
550
650
750

Figure 5B

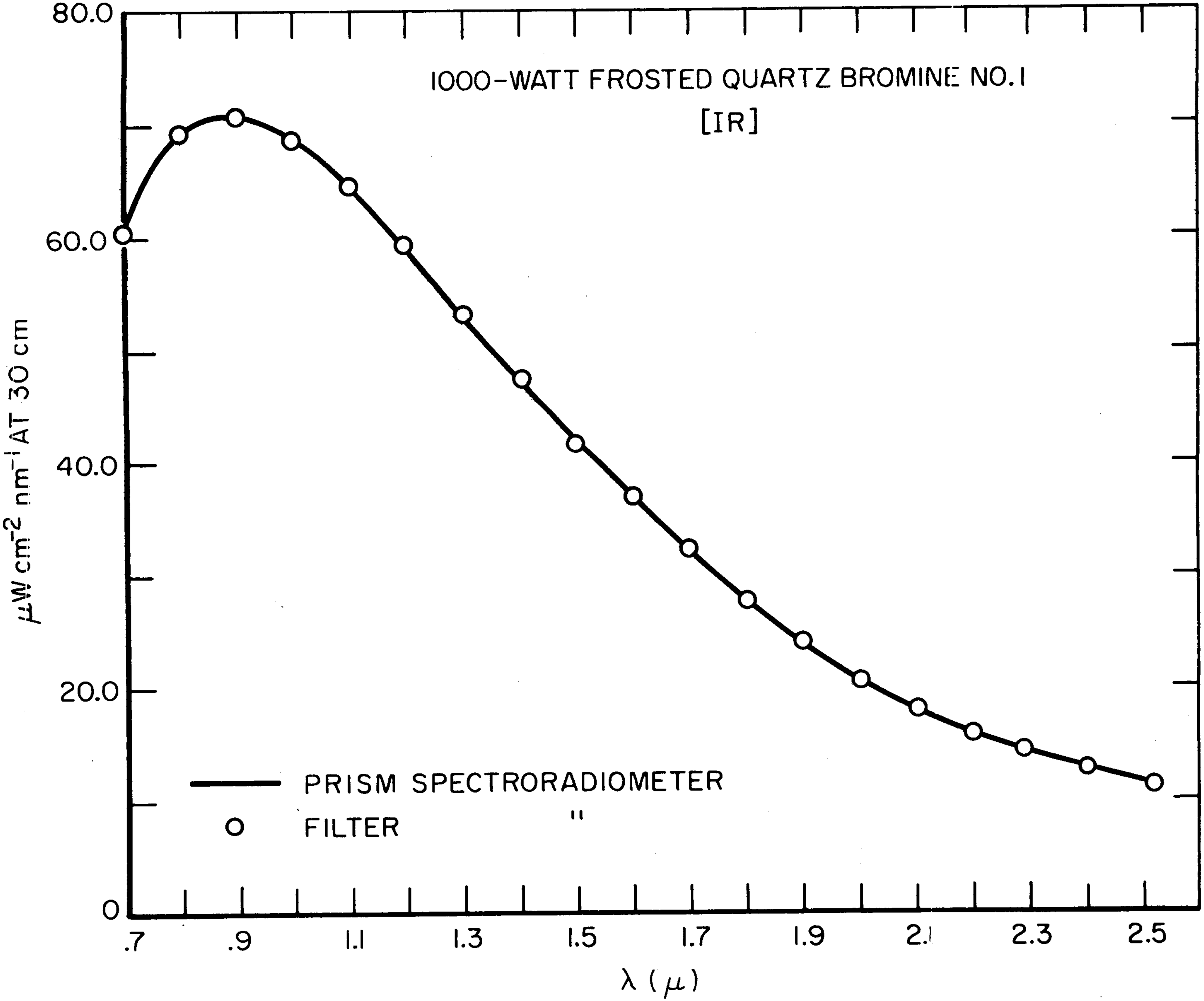
1000-WATT FROSTED QUARTZ BROMINE NO.1
[IR]
80.0
60.0
40.0
20.0
0
μW cm⁻² nm⁻¹ AT 30 cm
.7
.9
1.1
1.3
1.5
1.7
1.9
2.1
2.3
2.5
λ (μ)
PRISM SPECTRORADIOMETER
FILTER "

Figure 6A

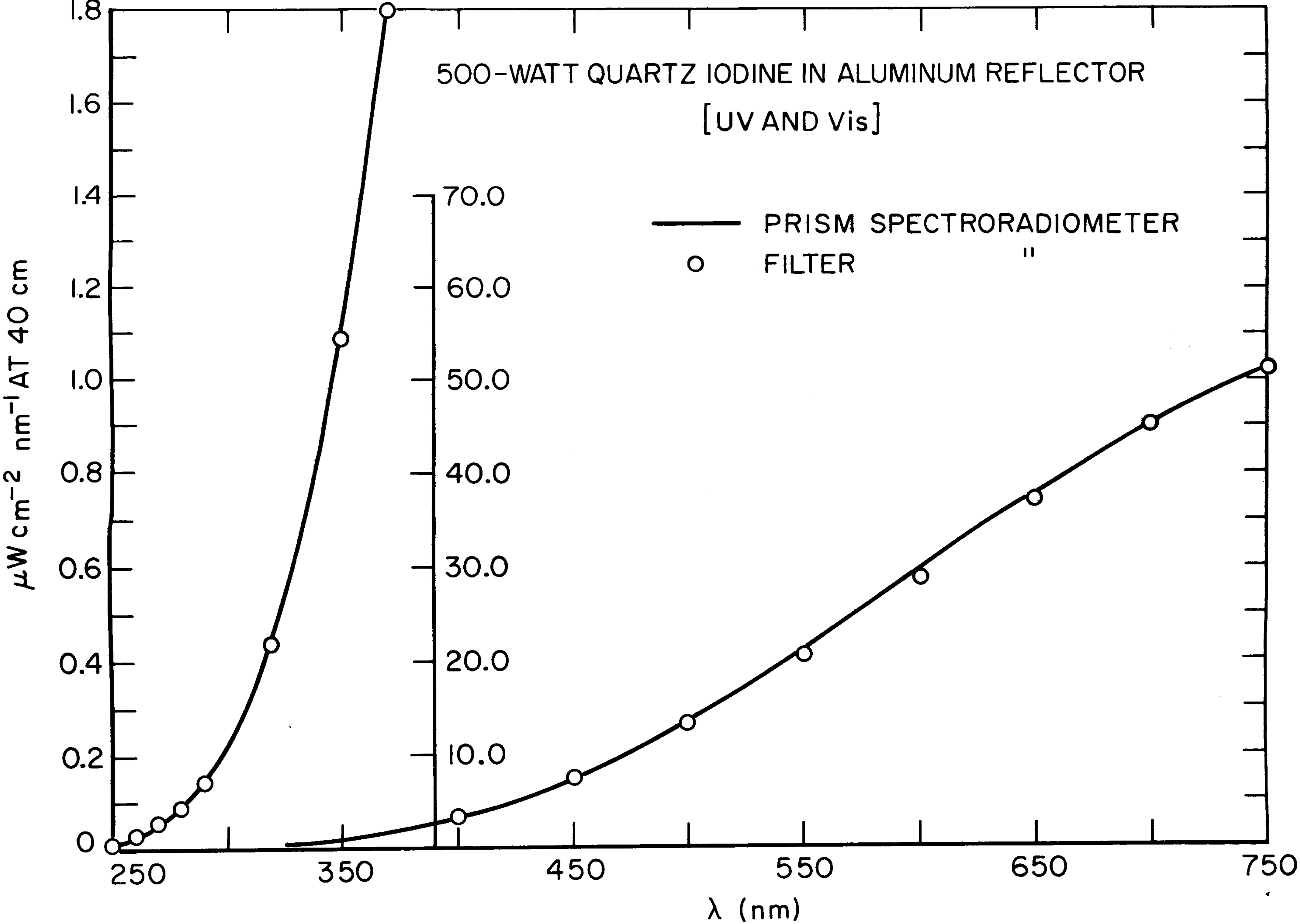
500-WATT QUARTZ IODINE IN ALUMINUM REFLECTOR
[UV AND Vis]
PRISM SPECTRORADIOMETER
FILTER "
μW cm⁻² nm⁻¹ AT 40 cm
λ (nm)
0
0.2
0.4
0.6
0.8
1.0
1.2
1.4
1.6
1.8
10.0
20.0
30.0
40.0
50.0
60.0
70.0
250
350
450
550
650
750

Figure 6B

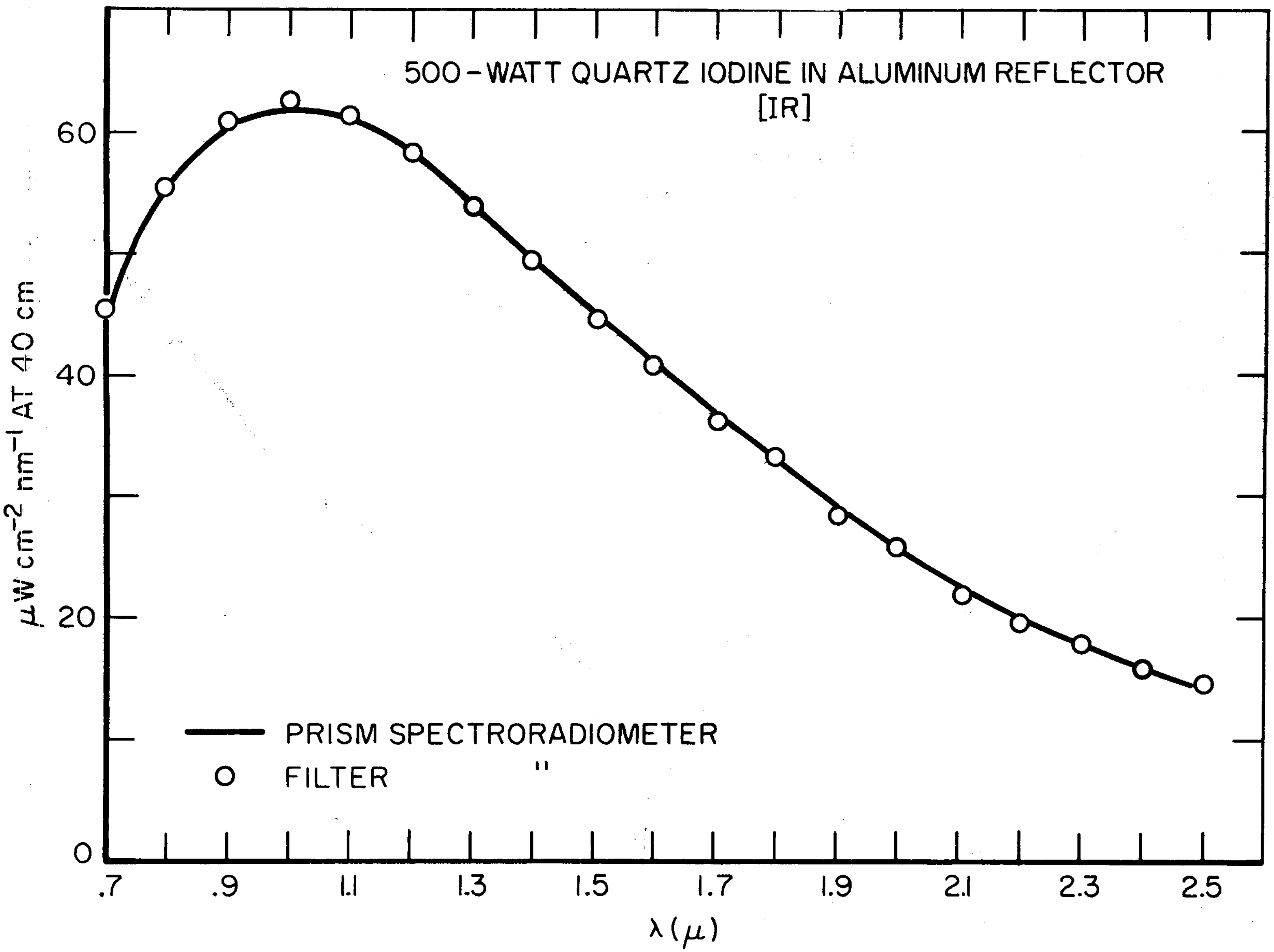
500-WATT QUARTZ IODINE IN ALUMINUM REFLECTOR
[IR]
PRISM SPECTRORADIOMETER
FILTER "
μW cm^{-2} nm^{-1} AT 40 cm
0
20
40
60
.7
.9
1.1
1.3
1.5
1.7
1.9
2.1
2.3
2.5
$\lambda (\mu)$

Figure 7A

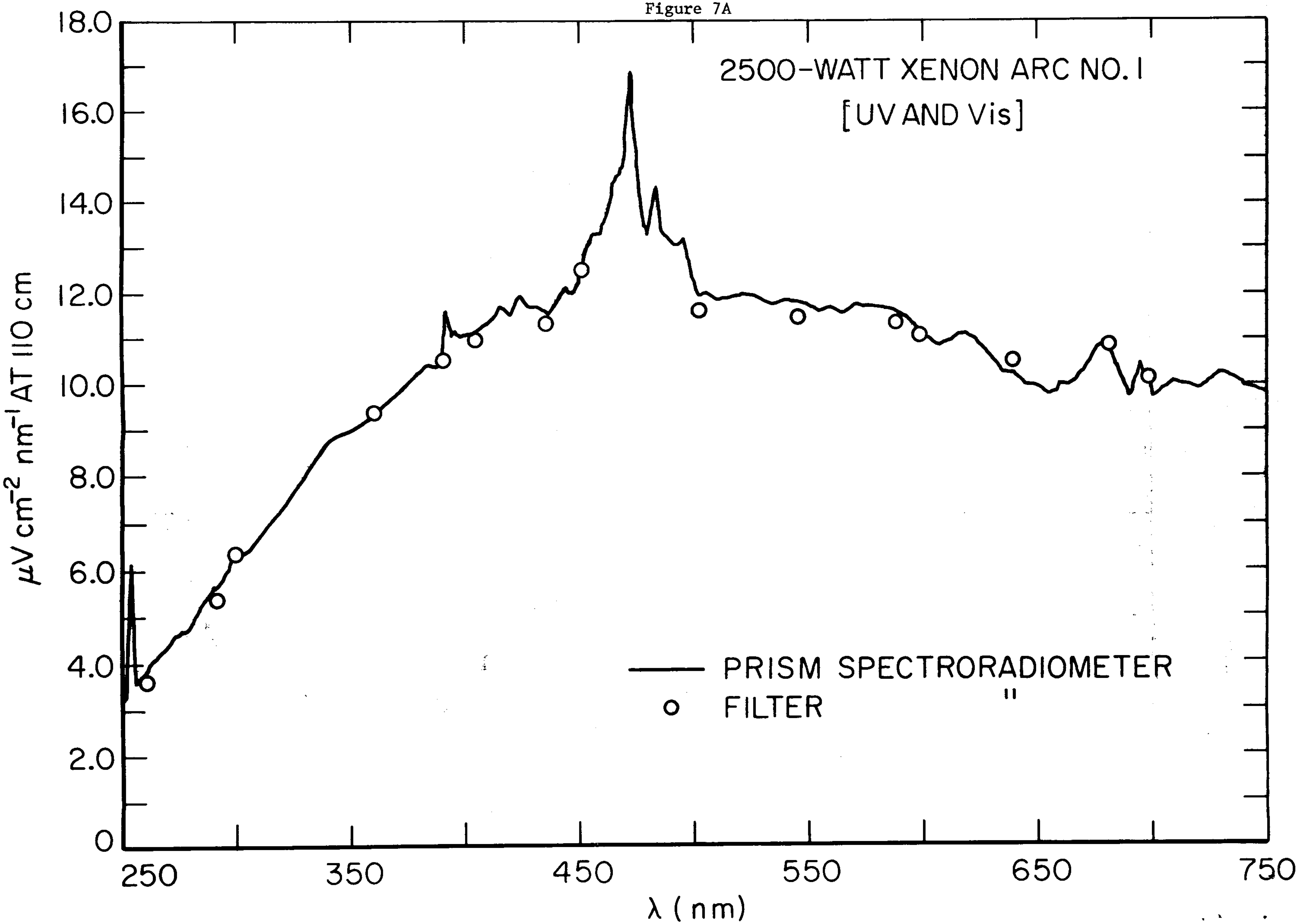

2500-WATT XENON ARC NO. I
[UV AND Vis]
PRISM SPECTRORADIOMETER
FILTER "
μV cm⁻² nm⁻¹ AT 110 cm
λ (nm)
18.0
16.0
14.0
12.0
10.0
8.0
6.0
4.0
2.0
0
250
350
450
550
650
750

Figure 7B

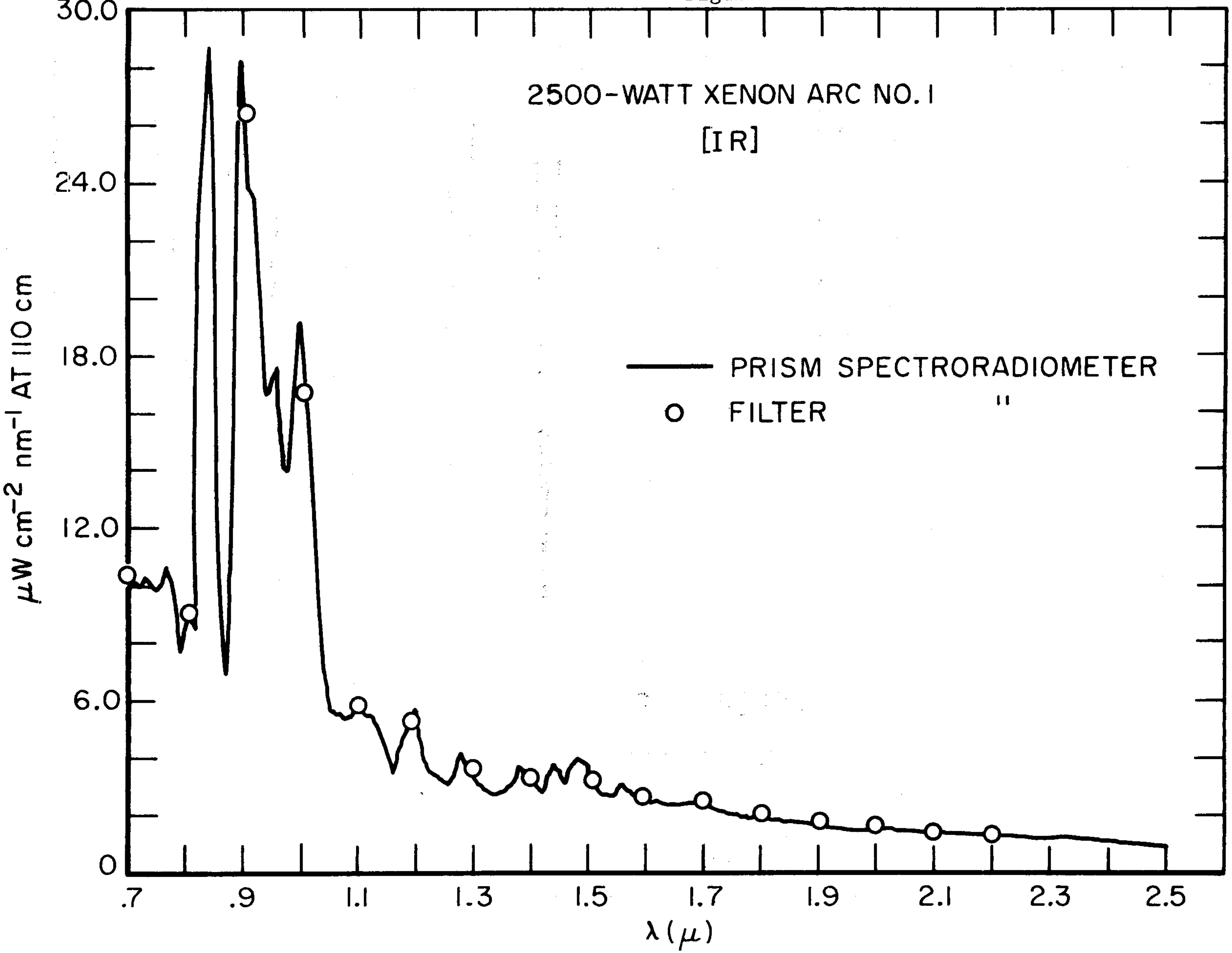

2500-WATT XENON ARC NO. 1
[IR]
PRISM SPECTRORADIOMETER
FILTER
"
30.0
24.0
18.0
12.0
6.0
0
μW cm⁻² nm⁻¹ AT 110 cm
.7
.9
1.1
1.3
1.5
1.7
1.9
2.1
2.3
2.5
λ (μ)

Figure 8A

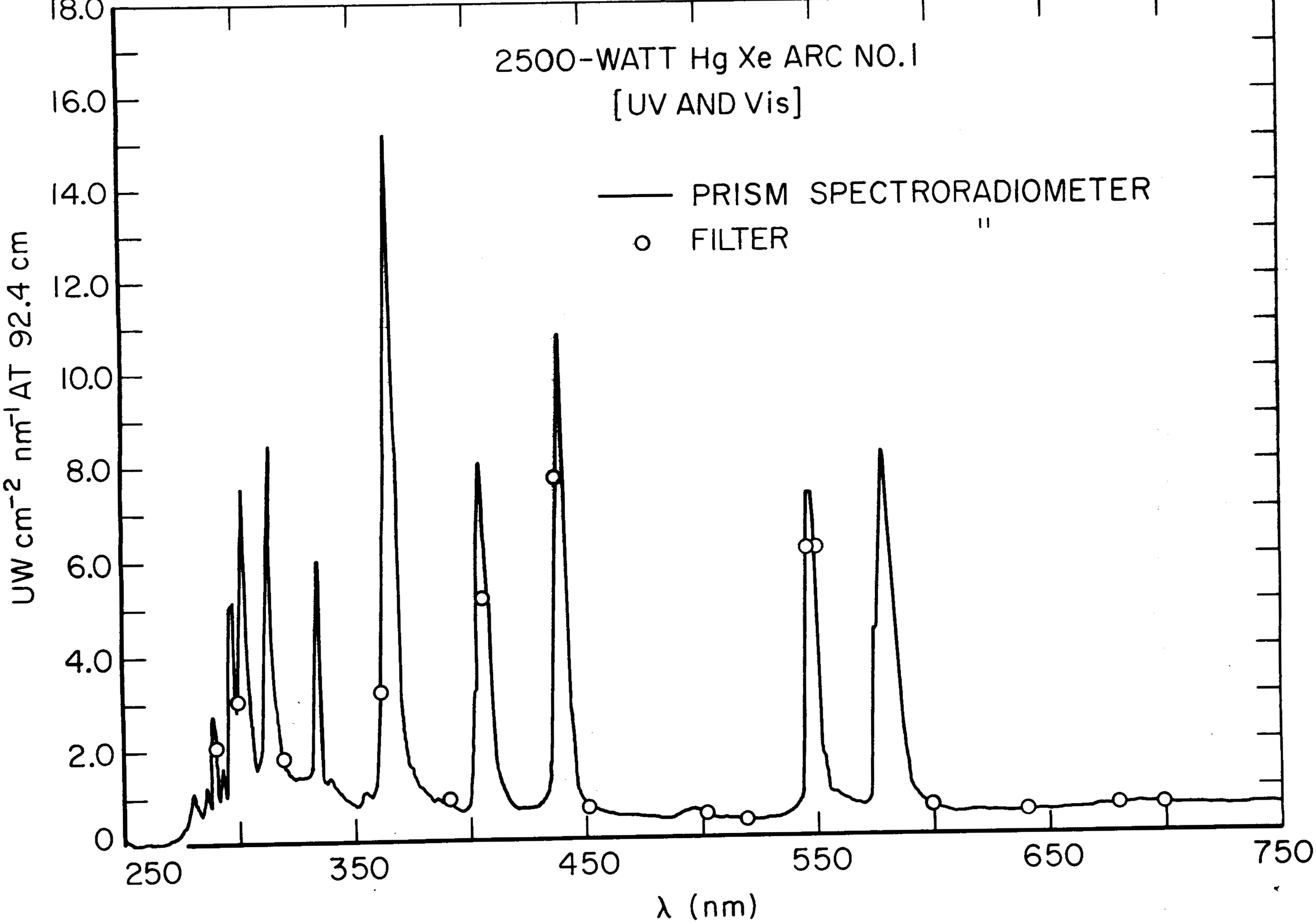
2500-WATT Hg Xe ARC NO.1
[UV AND Vis]
PRISM SPECTRORADIOMETER
FILTER "
UW cm^{-2} nm^{-1} AT 92.4 cm
λ (nm)
18.0
16.0
14.0
12.0
10.0
8.0
6.0
4.0
2.0
0
250
350
450
550
650
750

Figure 8B

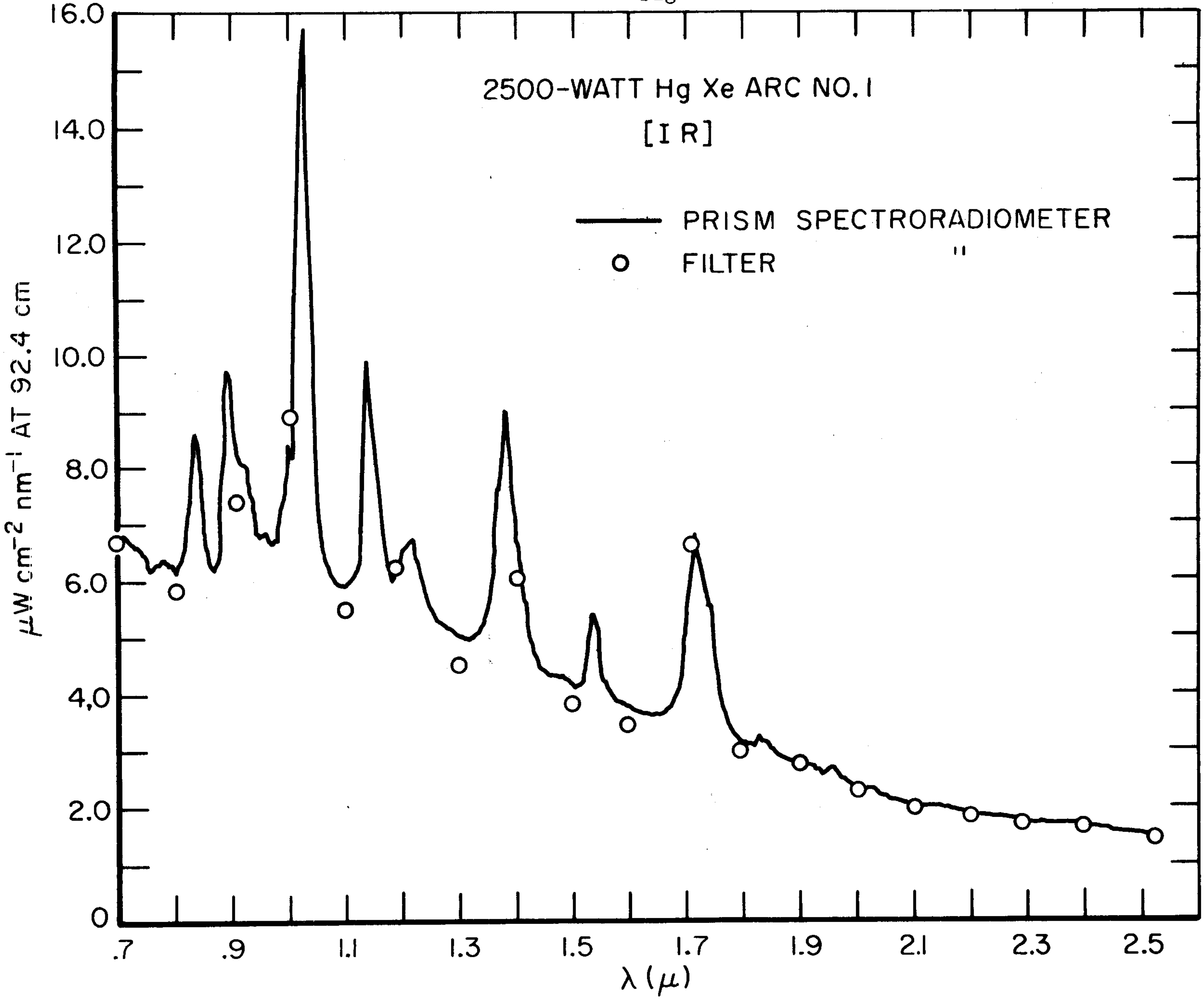
2500-WATT Hg Xe ARC NO. 1
[I R]
PRISM SPECTRORADIOMETER
FILTER "
$\mu W\ cm^{-2}\ nm^{-1}$ AT 92.4 cm
16.0
14.0
12.0
10.0
8.0
6.0
4.0
2.0
0
.7
.9
1.1
1.3
1.5
1.7
1.9
2.1
2.3
2.5
$\lambda\ (\mu)$

Figure 9A

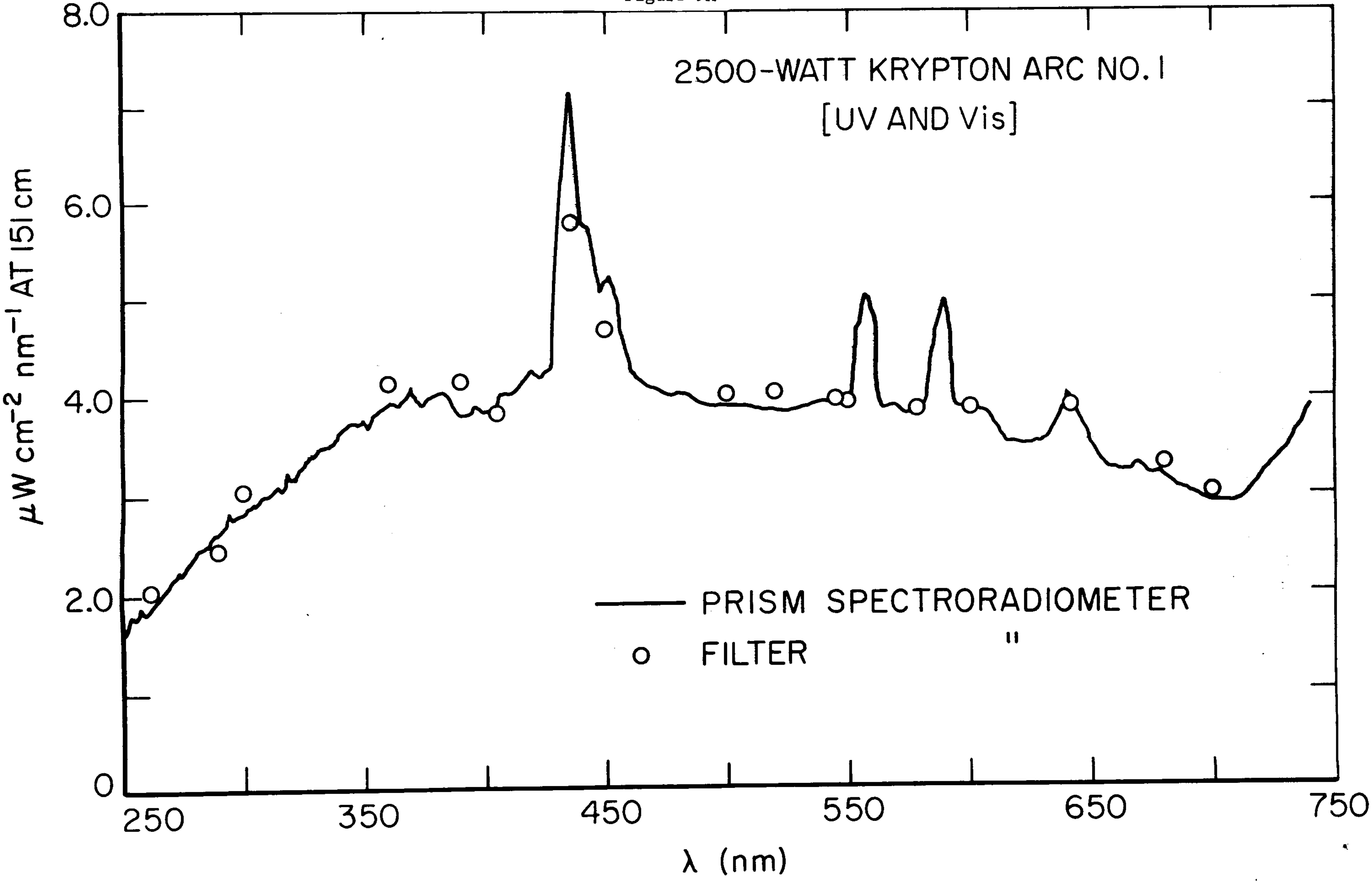
2500-WATT KRYPTON ARC NO. 1
[UV AND Vis]
PRISM SPECTRORADIOMETER
FILTER "
$\mu W\ cm^{-2}\ nm^{-1}$ AT 151 cm
8.0
6.0
4.0
2.0
0
250
350
450
550
650
750
λ (nm)

Figure 9B

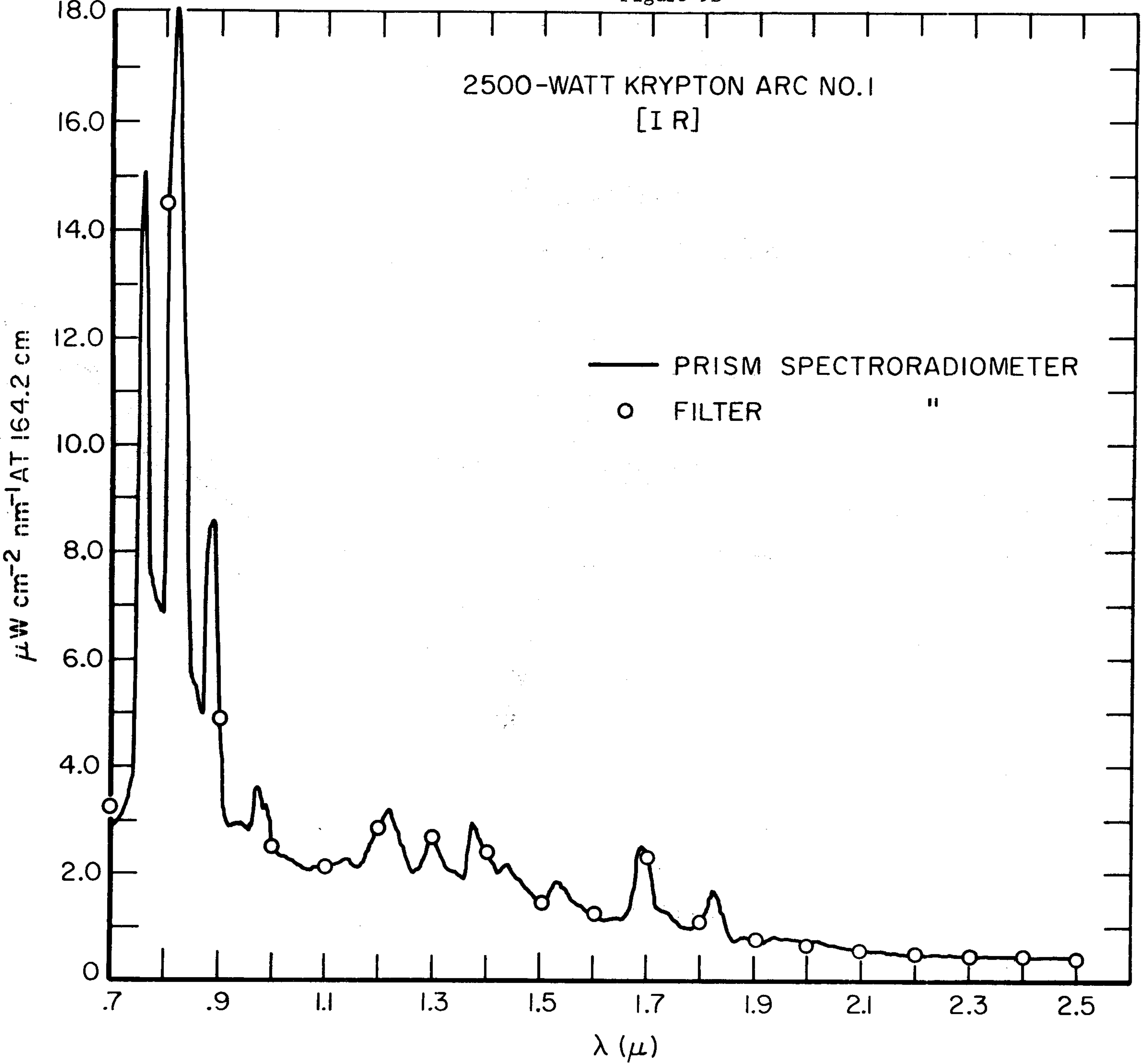

2500-WATT KRYPTON ARC NO.1
[I R]
PRISM SPECTRORADIOMETER
FILTER "
μW cm⁻² nm⁻¹ AT 164.2 cm
λ (μ)
18.0
16.0
14.0
12.0
10.0
8.0
6.0
4.0
2.0
0
.7
.9
1.1
1.3
1.5
1.7
1.9
2.1
2.3
2.5

Figure 10A

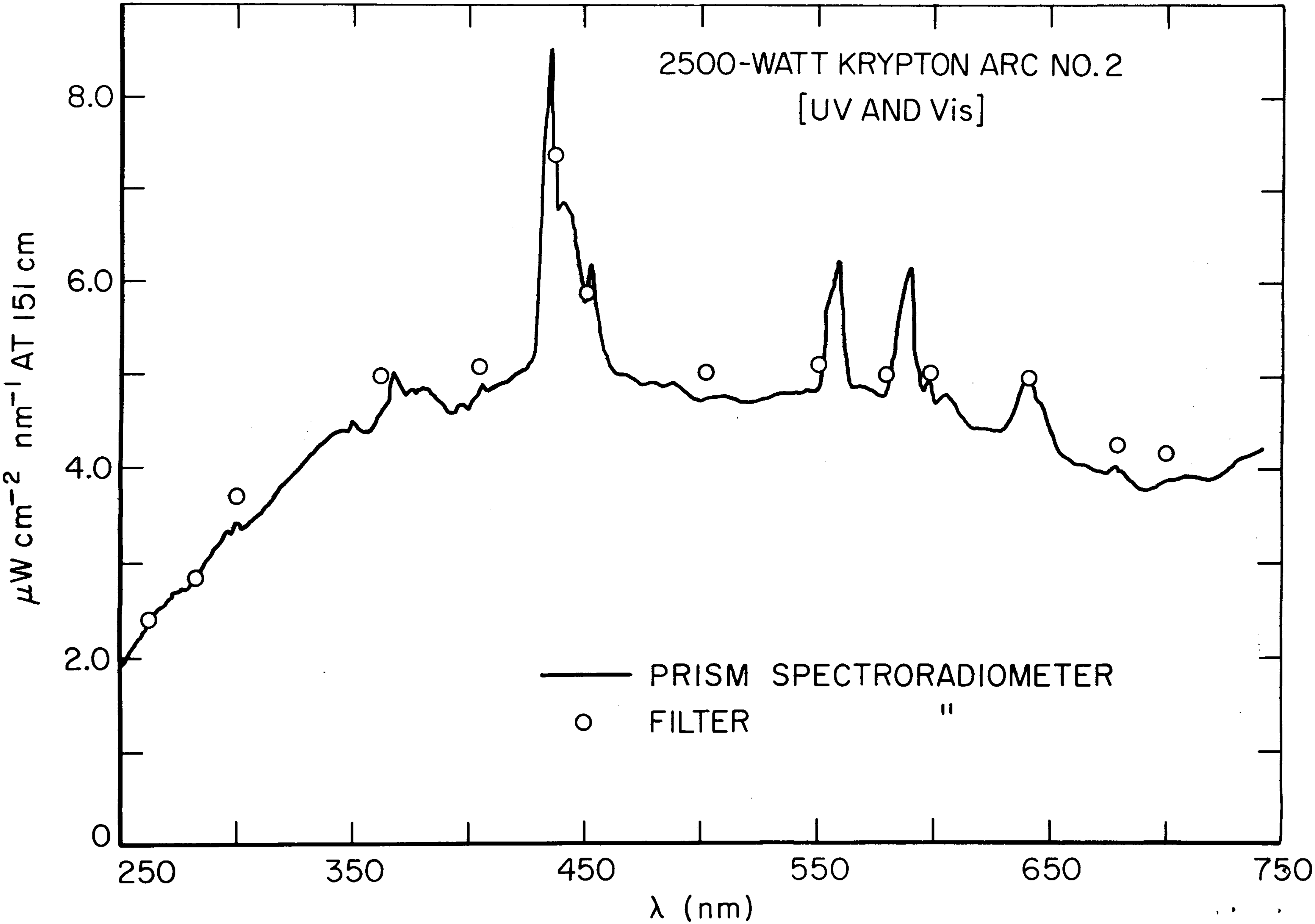
2500-WATT KRYPTON ARC NO. 2
[UV AND Vis]
PRISM SPECTRORADIOMETER
FILTER "
$\mu W\ cm^{-2}\ nm^{-1}$ AT 151 cm
8.0
6.0
4.0
2.0
0
250
350
450
550
650
750
λ (nm)

Figure 10B

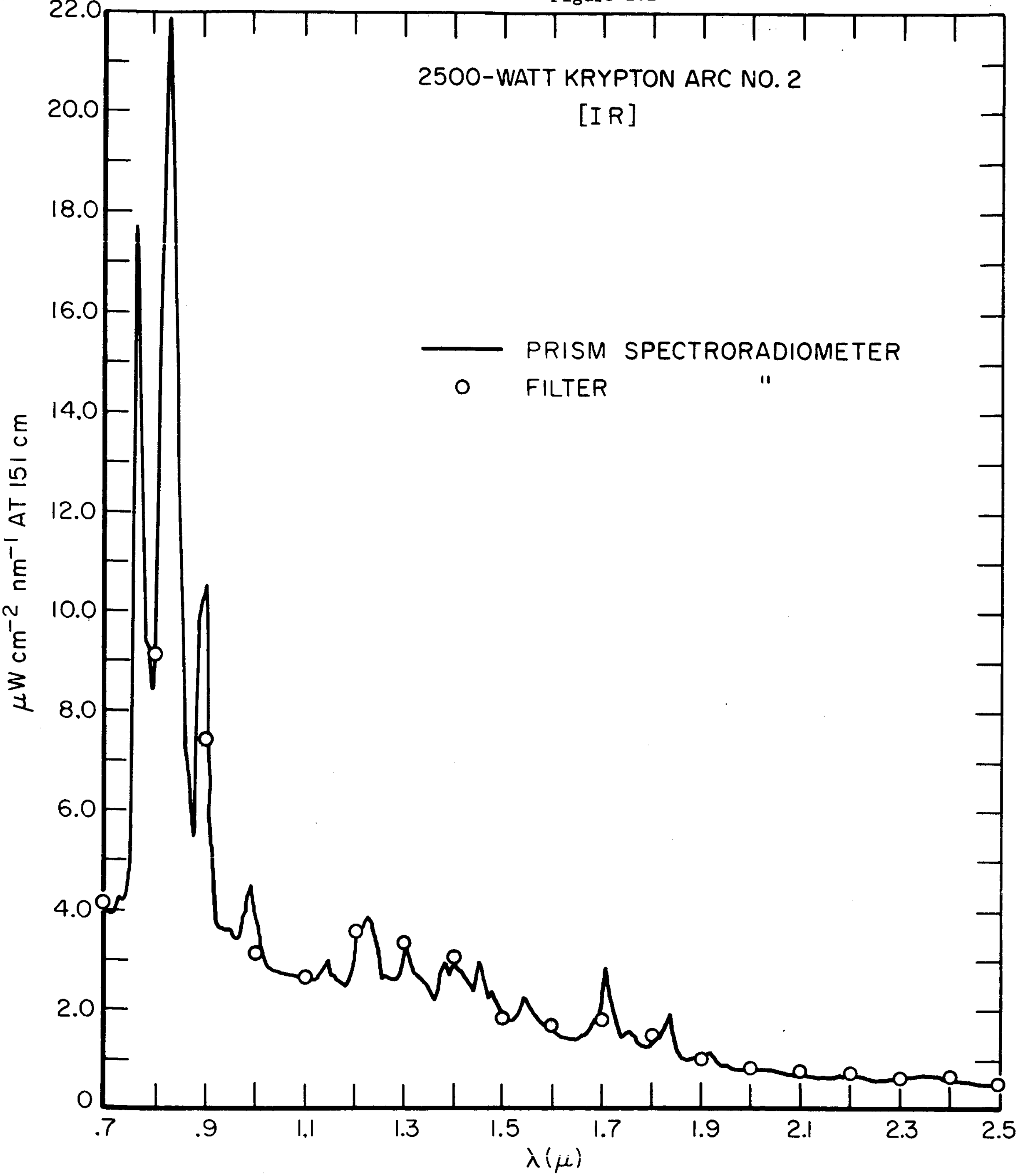
2500-WATT KRYPTON ARC NO. 2
[I R]
PRISM SPECTRORADIOMETER
FILTER "
$\mu W\ cm^{-2}\ nm^{-1}$ AT 151 cm
22.0
20.0
18.0
16.0
14.0
12.0
10.0
8.0
6.0
4.0
2.0
0
.7
.9
1.1
1.3
1.5
1.7
1.9
2.1
2.3
2.5
$\lambda(\mu)$